Impacts of Forced and Internal Climate Variability on Changes in Convective Environments Over the Eastern United States

Megan E. Franke[1], **James W. Hurrell**[1], **Kristen L. Rasmussen**[1], **Lantao Sun**[1]

[1]Colorado State University

Key Points:

- The signal of climate change in large-scale convective environments over the U.S. emerges from the internal variability in the late 1990's.
- Future convective environments over the eastern U.S. will be supportive of less frequent, less organized, but more intense storms.
- Large-scale internal climate variability could significantly enhance or suppress the changes due to anthropogenic climate change.

Corresponding author: Megan E. Franke, `megan.franke@colostate.edu`

Abstract

Hazards from convective weather pose a serious threat to the continental United States (CONUS) every year. Previous studies have examined how future projected changes in climate might impact the frequency and intensity of severe weather using simulations with both convection-permitting regional models and coarser climate and Earth system models. However, many of these studies have been limited to single representations of the future climate state with little insight into the uncertainty of how the population of convective storms may evolve. To thoroughly explore this aspect, a large ensemble of Earth system model simulations was implemented to investigate how forced responses in large-scale convective environments might be modulated by internal climate variability. Daily data from an ensemble of 50 simulations with the most recent version of the Community Earth System Model was used to examine changes in the severe weather environment over the eastern CONUS during boreal spring from 1870-2100. Results indicate that forced changes in convective environments were small between 1870 and 1990, but throughout the 21st century, convective available potential energy and atmospheric stability (convective inhibition) is projected to increase while 0-6 km vertical wind shear decreases. Internal climate variability can either significantly enhance or suppress these forced changes. The time evolution of bivariate distributions of convective indices illustrates that future springtime convective environments over the eastern CONUS will be characterized by relatively less frequent, less organized, but deeper, more intense convection. Future convective environments will also be less supportive of the most severe convective modes and associated hazards.

Plain Language Summary

Understanding to what extent climate change will alter severe weather is critical for planning and resilience. Moreover, natural variations in climate could either enhance or suppress climate change signals, so documenting the range of equally plausible future outcomes is important. Utilizing a large number of simulations from a climate model, we document projected changes in large-scale atmospheric conditions critical to severe weather from both climate change and natural variability. The impact of climate change on these environments became apparent late in the 20th century and will likely strengthen over the coming decades. Convective environments over the eastern U.S. will increasingly be supportive of less frequent, less organized, but more explosive storms due to increases in mid-level stability and positively buoyant energy, but slight decreases in vertical wind shear. However, such changes may be significantly modified by natural climate variability, resulting in a wide range of possible outcomes.

1 Introduction and Motivation

Few places around the globe experience extreme severe weather like the United States (U.S.). Particularly over the central and eastern U.S., the peak in severe weather is largely due to synoptic-scale interactions with the Rocky Mountains. During the boreal spring season, the Bermuda High, as well as the nocturnal Great Plains Low-Level Jet (GPLLJ), enhances a southerly flow of warm, moist air from the Gulf of Mexico into the Great Plains (Pitchford & London, 1962; Higgins et al., 1997; W. Li et al., 2011). This moist air, trapped by the mountains to the west, creates a strong gradient between the dry, western desert air and provides the necessary ingredients for high convective energy downstream. In addition, the terrain of the Rockies helps to produce a mid-level capping inversion as the hot, dry, mixed-layer air is advected off the elevated plateaus, which can then be further enhanced as the climatological westerly flow aloft descends the lee-side of the mountains (Carlson et al., 1983). This inversion suppresses convective activity and further facilitates the daily accumulation of convective energy increasing to very high levels. If the inversion is then broken, enhanced lifting and deep convection can occur.

In the year 2021 alone, 20 destructive meteorological events occurred in the U.S. each resulting in $1 billion or more of damages. Eleven of these events were due to severe weather and included hazards such as tornadoes, large hail, and strong winds (NCEI, 2021). Records from the National Climatic Data Center indicate that, over the last decade, the occurrence of billion-dollar severe weather events has more than doubled. Additionally, the Intergovernmental Panel on Climate Change (IPCC) has noted with high confidence that models consistently project changes in climate that support an increase in the frequency and intensity of severe weather (IPCC, 2021). As temperatures increase due to enhanced greenhouse gas concentrations, the air-column moisture content also increases, thus leading to an increase in convective available potential energy - a key ingredient for the development of severe weather. In the current climate, hazards associated with severe storms already threaten lives, infrastructure, and food and water supplies within the U.S. and elsewhere. With this in mind, an improved understanding of the causes of both near-term and longer-timescale variability in severe weather could aid in improving the accuracy of future predictions, as well as enhance resilience to severe weather outbreaks.

Due to their relatively small scale and intermittent occurrence, observing and collecting homogeneous records of severe weather events is difficult, especially when these events occur in relatively unpopulated or rural areas (Johns & Doswell, 1992; Brooks et al., 2003). To partially offset the lack of direct, long-term, and reliable observations of severe storm events, the severe weather research community has developed convective indices and covariate proxies that represent the thermodynamic and kinematic components of the local storm environment and are indicative of conditions favorable for severe weather events (Ludlam, 1963; E. N. Rasmussen & Blanchard, 1998; Craven & Brooks, 2004). Consideration of these diagnostic variables can aid in determining the historical occurrence and future probability of severe weather, including the frequency, intensity, and type, or mode, of convection.

Convective Available Potential Energy (CAPE) is a measure of the potential energy available for upward vertical motion in a storm environment, while Convective Inhibition (CIN) is indicative of the boundary layer stability, which inhibits upward vertical motion. Considerable prior research has investigated both the recent historical climatology as well as projections of the future evolution of these parameters. In general, these studies have shown that boreal spring CAPE is expected to increase substantially over the eastern continental U.S. (CONUS) by the end of the 21st century, largely as a result of an increase in specific humidity and warmer temperatures (e.g., Trapp et al., 2007, 2009; Diffenbaugh et al., 2013; Seeley & Romps, 2015; Hoogewind et al., 2017; K. L. Rasmussen et al., 2017; Chen et al., 2020; Lepore et al., 2021). Although less explored, the spatiotemporal evolution of boreal spring CIN is also consistent among previous studies, with increasing boundary layer stability (increasing CIN magnitudes) by 2100, particularly over the central CONUS (e.g., Hoogewind et al., 2017; K. L. Rasmussen et al., 2017; Chen et al., 2020; Lepore et al., 2021). While many of these studies have utilized large-scale climate models to explore future changes in these convective indices, others have taken a different approach by applying dynamical downscaling or the pseudo-global warming approach (Hoogewind et al., 2017; Chen et al., 2020). For example, K. L. Rasmussen et al. (2017) analyzed high-resolution convection-permitting simulations (Liu et al., 2017) using the regional Weather Research and Forecasting model (WRF; Skamarock et al., 2008) at 4 km resolution forced with ERA-Interim Reanalysis plus a climate change perturbation from climate model simulations to investigate how CAPE, CIN, and their subsequent convective populations may change in the future. In particular, they calculated end-of-century monthly anomalies of CAPE and CIN relative to the historical climatology (1976-2005) using a 19-model ensemble-mean from phase 5 of the Coupled Model Intercomparison Project (CMIP5; Taylor et al., 2012) under a strong, future emissions scenario. Their results are broadly consistent with the aforementioned studies, with increases projected in spring and summer CAPE and increasing magnitudes of CIN (in-

creased stability) over the eastern CONUS. Such findings suggest that in the future, weak to moderate storms will be less frequent because of increased stability, but the most intense storms will become more numerous (K. L. Rasmussen et al., 2017).

In contrast, there is less agreement on projected end-of-century changes in tropospheric wind shear, which is a key factor for storm organization, longevity, and severe weather development. For instance, Trapp et al. (2007), Diffenbaugh et al. (2013), and Ting et al. (2019) used a variety of Earth system models with RCP8.5 forcing and found a robust swath of decreasing wind shear over most of the CONUS during the boreal spring season, while Hoogewind et al. (2017) and Lepore et al. (2021) both found increasing wind shear over the western and central U.S. with decreasing shear over the eastern U.S. by 2100 also using Earth system models.

While changes in individual convective indices are useful for analyzing specific characteristics of severe storms, integrated measures of changes in storm environments, such as the product of CAPE and the wind shear between the surface and 6-km (S06), can provide a more complete spatiotemporal description of the convective environment. By definition, CAPES06 considers both the thermodynamic energy and the kinematic motion in a storm environment. As a result, increases in this variable could signify an increase in the frequency of significant severe storms relative to non-severe storms (E. N. Rasmussen & Blanchard, 1998; Brooks et al., 2003; Brooks, 2009). The historical climatology of warm-season CAPES06 produces a large-scale, spatially coherent pattern over the eastern CONUS, reflecting the climatology of the CAPE index (Brooks et al., 2003; F. Li et al., 2020). Simulations of future projections suggest that CAPES06 will mirror changes in CAPE. For instance, Seeley and Romps (2015) used a subset of climate models from the CMIP5, chosen based on their ability to reproduce a radiosonde climatology of severe storm environments, to compare 21st century changes in the frequency of environments favorable for severe weather using a CAPES06 threshold. In general, all four models produced changes for end-of-century CAPES06 that showed consistent spatial patterns with increases over the southern and central U.S. ranging from 50 to 180% of the historical climatology (Seeley & Romps, 2015).

Another approach has been to consider combinations of convective indices to determine the Number of Days with SEVere weather environments (NDSEV; Brooks et al., 2003). Previous studies agree that NDSEV will increase over much of the U.S. during the boreal spring season, but differences exist in the projected magnitudes of the increases. For instance, Trapp et al. (2007, 2009) and Diffenbaugh et al. (2013) find an increase of $\sim$3 days per season over the central and eastern CONUS by 2100 utilizing an Earth system model, whereas Hoogewind et al. (2017) found an increase of $\sim$10 days per season using a dynamical downscaling approach. Such discrepancies are likely a consequence of varying definitions used for the NDSEV parameter, contrasting time periods between the studies, as well as model grid-spacing and emission scenario differences.

The aforementioned studies have provided valuable insights and have set the foundation for the types of changes that are likely to be experienced in future convective environments during the boreal spring over the U.S. However, they primarily use either a small number of simulations from a single model, short integration periods ($\sim$30 years), or multi-model ensemble means with different emission scenarios and other model variations to compare changes in convective environments due to anthropogenic forcing. An additional and important perspective can be gained by utilizing a large ensemble approach from a single model, whereby many simulations of the future are run under the same radiative forcing scenario but are started from slightly different initial conditions. The significance of this approach arises from the presence of unpredictable, internal (or natural) climate variability, which results in a range of possible future outcomes, all of which can be considered a possible reality (e.g., Deser et al., 2012a). Internal variability is one of the largest factors of unavoidable uncertainty in regional climate projections and can either enhance or suppress a forced signal (Deser, 2020). It is important to note that each

simulation in a large ensemble contains a common response to the radiative forcing superimposed upon a different sequence of internal variability. In general, internal climate variability is larger in the extra-tropics than in the tropics and is relatively stronger compared to forced variability when examining climate change several decades into the future (Hawkins & Sutton, 2009; Deser et al., 2012a; Milinski et al., 2020), as has been done here.

Sub-seasonal to decadal variability is often associated with leading modes of climate variability. A handful of studies have examined the relationship between severe weather and modes of climate variability such as the El Niño Southern Oscillation (ENSO; Lee et al., 2013; Allen et al., 2015) and the Madden Julian Oscillation (MJO; Thompson & Roundy, 2013). Allen et al. (2015) found that fewer tornado and hail events occur over the central U.S. during El Niño events than during La Niña events. Thompson and Roundy (2013) showed that violent tornado outbreaks in the months March-May are more than two times more frequent during the second phase of the Real-time Multivariate MJO (RMM) index than during any other phases or during MJO inactivity. These results are critical in helping to both better understand the patterns of severe weather outbreaks as well as improve the skill for long-range seasonal predictions of severe weather events (Allen et al., 2015). However, how low-frequency, unforced climate variability modulates the convective mode (i.e. frequency and storm type), as well as the thermodynamic and kinematic environment critical for severe weather, has not been examined extensively to date, even though it is likely an important influence regionally.

As such, this study builds on the previous literature, specifically by taking advantage of a recently released large ensemble of simulations from the Community Earth System Model version 2.0 (CESM2; Danabasoglu et al., 2020), hereafter referred to as the CESM2-LE (Rodgers et al., 2021). Leveraging the CESM2-LE, which extends from 1870-2100, allows us to evaluate the temporal evolution of convective environments over a much longer, continuous-time record than has been examined before. Further, it allows us to robustly examine both the forced variability due to anthropogenic climate change, as well as the possible role of internal variability in modulating the forced signal over the coming decades. To our knowledge, these aspects related to severe weather environments over the U.S. have yet to be rigorously examined, and thus represent a novel aspect of the current study. An increased understanding of the possible combined effects of forced and internal variability on convective environments is important for ensuring that climate adaptation policies are based on the most complete, scientific information available (Deser, 2020; Mankin et al., 2020).

2 Methodology

We utilize simulation data from the CESM (Hurrell et al., 2013; Danabasoglu et al., 2020). The open-source CESM is unique in that it is both developed and applied to scientific problems by a large community of researchers. It is a critical infrastructure for the U.S. climate research community and is principally funded by the National Science Foundation (NSF) and managed by the U.S. National Center for Atmospheric Research (NCAR). Simulations performed with the CESM have made many significant contributions to climate research, ranging from paleoclimate applications (e.g., Otto-Bliesner et al., 2016) to contributions to the North American Multi-Model Ensemble (NMME; Kirtman et al., 2014) seasonal forecasting effort led by the National Oceanic and Atmospheric Administration (NOAA). Simulations with CESM have also been used extensively in both national and international assessments of climate science, including substantial contributions to version 6 of the CMIP (CMIP6; Eyring et al., 2016). The salient point is that CESM provides the broader academic community with a core modeling system to investigate a diverse set of earth system interactions across multiple time and space scales.

2.1 Model Information and Data

Daily data for specific humidity, column air temperature, near-surface (10-meter) wind speed, zonal and meridional winds, and geopotential heights were obtained from a large ensemble (LE) produced with the coupled CESM2 (Danabasoglu et al., 2020). The CESM2-LE uses the Community Atmosphere Model version 6 (CAM6), which is a 'low-top' model consisting of 32 vertical levels (a relatively coarse stratospheric representation) and a nominal 1° (1.25° in longitude and 0.9° in latitude) spatial resolution. To study the temporal evolution of the severe weather environment over the CONUS during boreal spring, 50 ensemble members were analyzed spanning 1870-2100. Each ensemble member used CMIP6 forcings over the historical record and a future (2015-2100) forcing of SSP3-7.0 (Rodgers et al., 2021), a medium-high emissions scenario resulting in approximately 7.0 Wm^{-2} in radiative forcing by the end of the 21st century (O'Neill et al., 2016; IPCC, 2021). This level of forcing is currently a policy-relevant target, and it is a more moderate forcing scenario than those analyzed in most of the aforementioned studies that have examined future changes in convective indices. An ensemble of this size and duration with a CMIP6 generation Earth system model provides an unprecedented opportunity to investigate the long-term evolution of large-scale convective environments, how it is impacted by forced variability, and to what extent the latter is influenced by internal climate variability.

2.2 Convective Parameters

The CESM2-LE simulations were used to compute several parameters to quantify the thermodynamic and kinetic characteristics of the large-scale storm environment across the U.S. Closely associated with the potential occurrence of deep convection is CAPE (Jkg^{-1}) (Doswell & Rasmussen, 1994; Riemann-Campe et al., 2009). This thermodynamic parameter is formally defined as the vertical integral of buoyancy from the level of free convection (LFC) to the equilibrium level, making it suitable to diagnose conditional instability and potential updraft strength (Holton & Hakim, 2013). We have chosen to use the most-unstable CAPE in the lowest 3000 meters to ensure that our analysis captures potentially elevated convection, as well as the maximum instability (Rochette et al., 1999).

The CIN (Jkg^{-1}) is equal to the negative buoyancy, or the negative work done by the atmospheric boundary layer as a parcel ascends from the surface, through the stable layer, and to the LFC (Colby, 1984; E. N. Rasmussen & Blanchard, 1998; Riemann-Campe et al., 2009). It is routinely analyzed to evaluate the stability of the local atmosphere and the potential suppression of convective motions. As CIN is the amount of energy an air parcel needs to overcome in order to reach the LFC, it is commonly referred to as a negative value (i.e., more negative values mean more convective inhibition or more stability), but will be discussed here as changes in magnitude.

To explore the kinematic components of the convective environment, we used the difference in the bulk vertical wind shear from 10 meters above ground level to 6-km (∼525 hPa) altitude, known as S06 (ms^{-1}). Past work suggests that while lower-level wind shear is important for tornadic environments, S06 is one of the best indices for determining storm type and organization (E. N. Rasmussen & Blanchard, 1998; Weisman & Rotunno, 2000; Brooks et al., 2003). Large values of S06 are indicative of stronger mid-level rotation such as single-celled thunderstorms. In addition, higher S06 allows for increased organization for storm dynamics such as a tilted updraft, which is necessary to displace the area of upward vertical motion from the downward vertical motion. This increases the potential for the storm to form a mesocyclone and develop into a supercell, which is typically accompanied by severe weather hazards. Sufficient S06 is also essential for multi-cell organized systems, such as squall lines, as it helps to counteract the low-level circulation induced by the cold pool (Rotunno et al., 1988). As a cold pool is produced

by evaporative cooling near the surface, new cells are triggered along the gust front. The triggering and subsequent growth of these new cells are highly dependent on the amount of low-level wind shear, making it crucial to the longevity of a multi-cellular organized system.

A covariate convective index used here is the product of CAPE and S06, or CAPES06 (m^3s^{-3}). Previous research has demonstrated the effectiveness of CAPES06 to help discriminate between significant severe storms and less severe storms (E. N. Rasmussen & Blanchard, 1998; Craven et al., 2002; Brooks et al., 2003; Brooks, 2009; Seeley & Romps, 2015). As CAPES06 takes into account two of the most necessary components for convection, the thermodynamic energy and the vertical kinematic structure, high values of this parameter are indicative of increased storm organization and higher updraft velocities. Historically, soundings from days with the most severe storms exhibited high values in this index (e.g., E. N. Rasmussen & Blanchard, 1998; Brooks et al., 2003; Brooks, 2009).

Finally, to convey the integrated effects of the convective indices, changes in NDSEV are also examined. Following the definitions used in past studies (Brooks et al., 2003; Trapp et al., 2007; Gensini & Ashley, 2011; Hoogewind et al., 2017), a day is counted as a severe weather day when CAPE $\geq$ 100 Jkg^{-1}, CIN $\geq$ -100 Jkg^{-1}, S06 $\geq$ 5 ms^{-1}, and CAPES06 $\geq$ 10,000 m^3s^{-3}. Then, the sum of the number of days throughout the boreal spring season that meet the criteria are obtained to provide an estimate of the potential number of severe weather days per season.

This study will focus primarily on the eastern CONUS region outlined in Fig. 1, which is a highly active region for intense convection. Note, however, that the ocean regions are masked from the analysis so that the focus is on convective indices over land only. We define the spring season as March through June (MAMJ), as this period captures the months when storms are most frequent and violent over the eastern CONUS (Kelly et al., 1985; Brooks et al., 2003; Gensini & Ashley, 2011; F. Li et al., 2020). Later into the summer season, the temperature and moisture gradients in this region are weaker, and the jet-stream begins to shift north, resulting in an overall northward shift in convective activity.

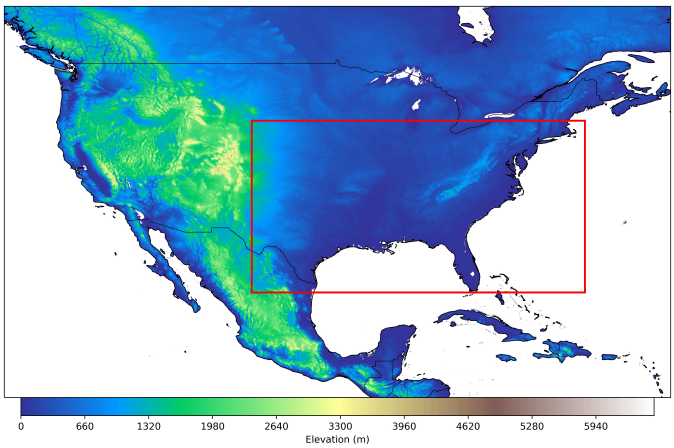

Figure 1. Red box highlights the eastern CONUS domain used for this study. Latitude bounds are between (25°N and 43°N) and longitude bounds are between (-104°W, -69°W).

2.3 Verification

To verify that the CESM2-LE is a viable tool for the analysis of large-scale convective environments, the fifth-generation global climate reanalysis (ERA5; Hersbach et al., 2020) from the European Centre for Medium-Range Forecast (ECMWF) was used for model validation. Previous studies have found ERA5 to be reliable in capturing the spatiotemporal climatology of convective environments (Taszarek et al., 2021). In particular, F. Li et al. (2020) conducted a climatological analysis of severe local storm environments over North America using ERA5 compared to CAM6 simulations of the historical period. They confirmed the validity of ERA5 against 69 radiosonde observations over the CONUS region with twice daily raw soundings and further confirmed the fidelity of CAM6 against ERA5. This is important because, relative to its predecessor CAM5 (Neale & Gettelman, 2012), CAM6 underwent significant modifications to the physical parameterization suite. Updates to the Zhang and McFarlane (1995) deep convection and orographic drag parameterizations were implemented into CAM6, along with the two-moment prognostic cloud microphysics from Gettelman and Morrison (2015). Additionally, the Cloud Layers Unified by Binormals (CLUBB; Golaz et al., 2002) replaced schemes for cloud macrophysics, boundary layer turbulence, and shallow convection previously used in CAM5, all of which are key parameterizations for modeling convection.

The MAMJ CAPES06 climatology from ERA5 (left) and the ensemble-mean climatology from CESM2-LE (right) is shown in Fig. 2 over the CONUS region. There is strong agreement between the CESM2-LE and ERA5 during 1980-2019, indicating that the model successfully captures the mean spatial characteristics of CAPES06 over the past 40 years. Although not shown, similarly strong agreement is found between ERA5 and CESM2-LE for the climatologies of the other convective indices (CAPE, CIN, and S06).

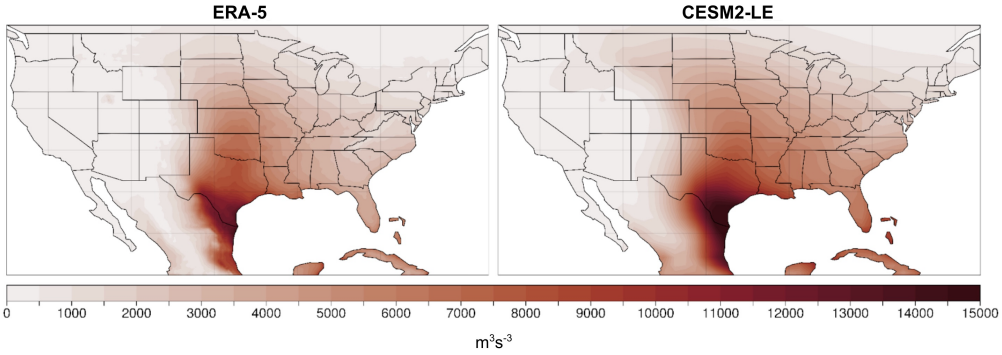

Figure 2. MAMJ CAPES06 (m^3s^{-3}) climatology for ERA5 reanalysis (left) and the CESM2-LE ensemble-mean (right) for the 1980-2019 period.

To further examine the fidelity of the CESM2-LE, we investigated the relationship between CAPES06 and ENSO, the largest driver of interannual changes in weather and climate over much of the globe (Ropelewski & Halpert, 1986; Dai et al., 1997; Allen et al., 2015; Dai & Wigley, 2000). The regression of boreal spring CAPES06 from ERA5 onto the observed Niño3.4 index over 1980-2019 is shown in Fig. 3 on the left, compared to the same quantity from the CESM2-LE over 1870-2019 on the right. Notably, CESM2-LE captures the main changes in CAPES06 associated with ENSO, including large-scale decreases in CAPES06 over the eastern CONUS during El Niño, with increases over the western CONUS. Since this study utilizes a large ensemble, many more El Niño events are sampled from the CESM2-LE data than from ERA5, resulting in more coherent spa-

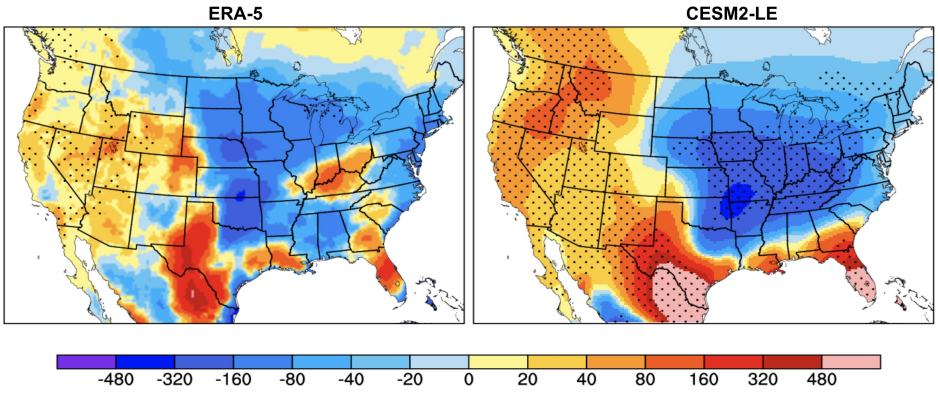

Figure 3. Regression of CAPES06 onto the ENSO index for one standard deviation over the MAMJ season from ERA5 reanalysis (1980-2019; left) and the CESM2-LE (1870-2019; right). Stippling on ERA5 shows the 95% statistical significance based on the Students T-test. Stippling on CESM2-LE indicates where 45 of the 50 members have the same sign.

tial patterns. This relationship is consistent with other studies that have investigated the role of ENSO on severe weather outbreaks over the U.S. during the March-May season (e.g., Lee et al., 2013; Allen et al., 2015). The results in this section, combined with the findings of earlier studies (e.g., F. Li et al., 2020), give us confidence in using the CESM2-LE to examine past and future changes in convective environments over the CONUS, as well as the variations driven by internal modes of climate variability (e.g., Capotondi et al., 2020; Rodgers et al., 2021).

3 Results

3.1 Ensemble Mean (Forced Changes)

The historical and future time evolution of the selected convective indices from 1870-2100 for the boreal spring season averaged over the eastern CONUS (Fig. 1) are shown in Fig. 4. The time series are expressed as seasonal anomalies relative to the 30-year base period 1971-2000. The forced component of climate change is given by the ensemble-mean of the CESM2-LE, represented by the solid black line, and the time evolution of individual ensemble members are depicted by the light gray lines. While considerable run-to-run, interannual and decadal variability is evident in individual ensemble members, the forced response in convective indices show minimal change from 1870 until about 1990, deviating little from the 30-year baseline climatologies. However, right around the year 2000, forced changes in convective environments become apparent and exhibit clear departures from the historical climatological values throughout the current century. For instance, ensemble-mean values of CAPE steadily increase throughout the 21st century, exceeding the historical climatological values by nearly 400 Jkg^{-1} by 2100 (Fig. 4a), while the forced change in S06 becomes more negative. Specifically, anomalies in S06 reach approximately -2 ms^{-1} by 2075, then remain near that level through the remainder of the century (Fig. 4b).

The time evolution of CAPES06 (Fig. 4c) exhibits behavior similar to that of CAPE, with an almost linear increase from 2000 of ~3500 m^3s^{-3} above the historical climatology by 2100. The time history of CIN also shows little deviation until this century, when it exhibits a steady decrease in magnitude to approximately -18 Jkg^{-1} by 2100 (Fig. 4d). These results show that changes in convective environments due to anthropogenic forcing through the end of this century are prominent and robust in CESM2-LE, as they are

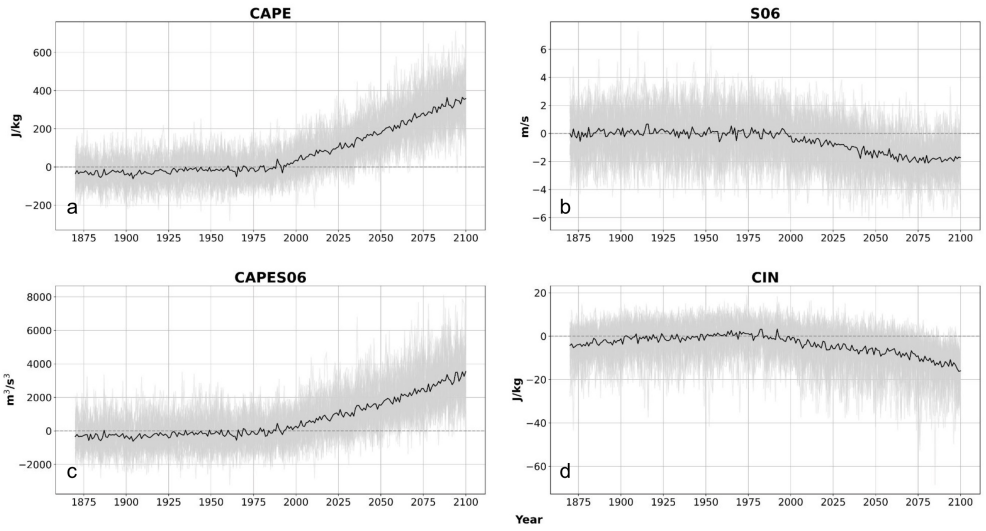

Figure 4. Time series of convective indices from 1870-2100 for (a.) CAPE (Jkg^{-1}), (b.) S06 (ms^{-1}), (c.) CAPES06 (m^3s^{-3}), and (d.) CIN (Jkg^{-1}) over the eastern CONUS region. The 50-member ensemble-mean (black) is superimposed on individual members (light grey).

reflected in nearly all of the 50 members of the ensemble (light grey lines in Fig. 4). Few previous studies have been able to estimate the continuous-time evolution of changes in these convective indices. One example is Diffenbaugh et al. (2013), who leveraged the CMIP5 to take regional averages over eastern CONUS for CAPE, S06, and NDSEV from 1960-2100 using RCP8.5. Furthermore, Trapp et al. (2009) used a five-member ensemble from the Community Climate System Model version 3 (CCSM3) to take various regional averages in areas over the CONUS that frequently encounter severe weather, including the southeast, Midwest, and the southern and northern Great Plains. This was done for the same indices as Diffenbaugh et al. (2013) but from 1950-2100. In general, the trends and magnitudes of the changes in these indices are in agreement with the changes expressed in Fig. 4, especially over the southern Plains and southeast CONUS, as seen in Trapp et al. (2009). The principal point is that convective environments over the eastern CONUS during the boreal spring are likely to undergo substantial departures from the historical record over this century (Fig. 4), moving toward higher convective energy, more stability, and less kinematic support for the production of hazards associated with severe weather.

To evaluate the spatial character of these changes over the CONUS, epoch differences for future 30-year periods relative to the 1971-2000 baseline climatology are shown in Fig. 5. By 2100, the CESM2-LE projects spatially coherent forced changes in convective environments relevant to the frequency and intensity of severe weather. Over the next few decades (2021-2050), increases in CAPE are largest near the Gulf coast and are positive across the entire CONUS (Fig. 5a). These changes in CAPE are projected to strengthen throughout the rest of this century, primarily over the eastern CONUS and southern Plains (Trapp et al., 2007; Diffenbaugh et al., 2013; Seeley & Romps, 2015; Hoogewind et al., 2017; K. L. Rasmussen et al., 2017; Chen et al., 2020; Lepore et al., 2021). As CAPE is related to the maximum potential updraft within a thunderstorm by $w_{max} = \sqrt{2CAPE}$ (Holton & Hakim, 2013), projections of higher CAPE imply that, on average, future storms will have stronger updrafts, resulting in deeper, more explosive convection than storms during the reference period (1971-2000). Additionally, it was shown by Dougherty and Rasmussen (2021) that updraft intensities increased in flood-producing storms in CONUS

simulations, further supporting the hypothesis that increasing CAPE results in an increased risk for severe weather. The spatial patterns in these changes also highlight the continued influence of the GPLLJ advecting warm, moist air into the Plains and east of the Rocky Mountains (e.g., Carlson et al., 1983).

Epoch differences in boreal spring wind shear reveal a large and spatially coherent east-west swath of decreasing S06 over the entirety of the CONUS, increasing in magnitude with time in Fig. 5b (Trapp et al., 2007, 2009; Diffenbaugh et al., 2013; Hoogewind et al., 2017; Lepore et al., 2021; Ting et al., 2019). The greatest changes appear in the northeast, with smaller decreases over the southern CONUS. Sufficient shear is imperative to the internal dynamics of a thunderstorm since it promotes vertical storm-scale rotation and assists in sustaining the updraft (Weisman & Rotunno, 2000; Trapp et al., 2007), which are important ingredients for tornadogenesis, large hail formation, and damaging outflow winds at the surface. Additionally, storm environments characterized by strong vertical wind shear are more likely to be organized, last longer, and become self-sustaining systems (e.g., Lilly, 1979; Rotunno, 1981; Klemp, 1987; Weisman & Rotunno, 2000). For these reasons, decreases in shear with time indicate that increasingly fewer thunderstorms will have the support necessary for the most hazardous and severe storms to form, including organized mesoscale convective systems (MCS).

To further diagnose the projected changes in S06, the changes of zonal and meridional winds near the surface and at 6-km were also analyzed. Future projections of surface winds do not reveal spatially coherent changes over the next century, but the zonal winds aloft indicate substantial departures from the historical record. In particular, nearly all of the CESM2-LE members project decreases in upper-level westerly winds over the CONUS during the boreal spring season that increase in magnitude with time. The causal mechanisms of these zonal wind changes are being explored further, but preliminary results suggest a connection to projected future changes in tropical rainfall patterns (not shown).

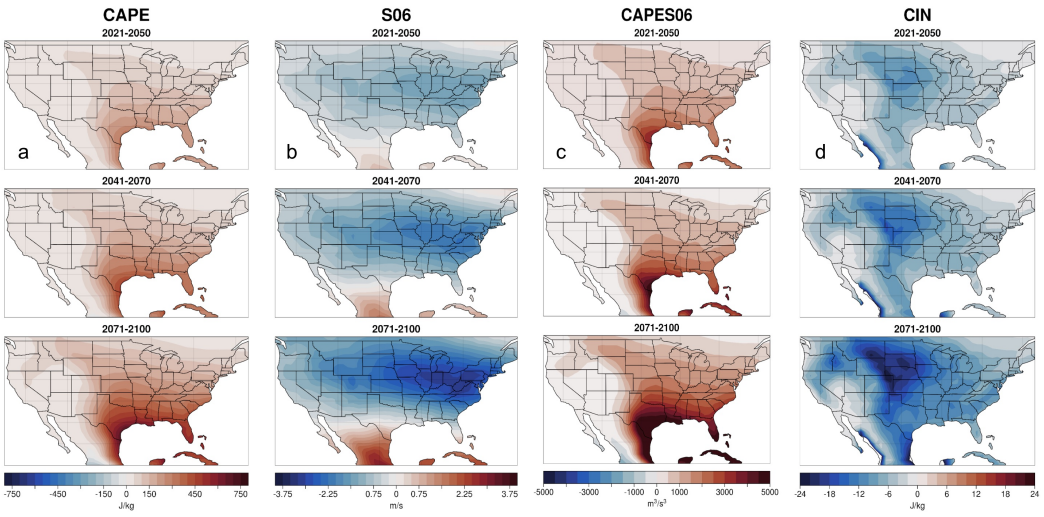

Figure 5. Epoch differences from the 1971-2000 baseline period for early (2021-2050), mid (2041-2070), and end-of-century (2071-2100) convective indices during MAMJ for (a.) CAPE (Jkg^{-1}) (b.) S06 (ms^{-1}) (c.) CAPES06 (m^3s^{-3}) and (d.) CIN (Jkg^{-1})

The projected spatial characteristics of changes in CAPES06 (Fig. 5c) are similar to those highlighted by (Seeley & Romps, 2015), who leveraged four climate mod-

els, archived from CMIP5 and forced with two different emission scenarios, to compare the end-of-century projections of CAPES06 over the U.S. Overall, their findings, as well as ours, show spatial patterns of boreal spring CAPES06 that are dominated by the changes in CAPE (Fig. 5a), characterized by a coherent increase with time over the eastern CONUS. Although the decreases in S06 suggest that there would be less support for storm organization and dynamics, some studies speculate that the large-scale increases in CAPE will make up for the diminishing S06 (Trapp et al., 2007, 2009). The main point is that CAPES06 is expected to undergo substantial increases by the end of this century, suggesting convective environments over the southeastern U.S. will be supportive of a higher ratio of significant severe versus non-severe storms.

However, this hypothesis does not take into account the increasing magnitude of CIN that represents the negative buoyancy that parcels need to overcome in order to realize their CAPE (K. L. Rasmussen et al., 2017). Despite enhanced CAPE values in a future climate, weak to moderate storms may be less frequent due to enhanced stability (i.e. CIN) that requires more lifting or heating to overcome. Changes in the forced component of CIN projected by the CESM2-LE are characterized by decreases over the central and northern Great Plains that increase in magnitude throughout this century, reaching approximately -18 Jkg^{-1} by 2100 (Fig. 5d). Such changes are indicative of a more stable or "capped" atmosphere. If strong enough (CIN < -200 Jkg^{-1}), this stability could potentially inhibit convection completely. On the other hand, there is the possibility that there is moderate CIN (-50 Jkg^{-1} > CIN > -200 Jkg^{-1}), allowing for an accumulation of CAPE that once released, could produce explosive convection. Globally, this is commonly observed in convective environments in the vicinity of large mountain ranges such as the Rockies and the Andes, as discussed in the introduction (Zipser et al., 2006; K. L. Rasmussen & Houze, 2011; K. L. Rasmussen et al., 2014; K. L. Rasmussen & Houze, 2016). The juxtaposition of the terrain-induced mid-level capping inversion with the warm, moist air allows for the modulation of CAPE by CIN until convective initiation occurs and intense convection is then able to develop. It is also evident in the spatial patterns (Fig. 5) that by the end of the century, the areas of maximum stability are not collocated with the areas of maximum convective energy. Therefore, since CIN is minimized over the Great Plains, while CAPE is maximized over the eastern U.S., the future frequency of convection in the Great Plains is, on average, likely to be less than the current climate but still vigorous due to increased stability, while convective frequency over the eastern U.S. is likely to be slightly less reduced, but more intense when it does occur as a result of the increased and accumulated CAPE. Overall, these changes are in agreement with previous studies using both Earth system models (Hoogewind et al., 2017; Lepore et al., 2021) and dynamical downscaling or a pseudo-global warming approach, such as K. L. Rasmussen et al. (2017) and Chen et al. (2020), projecting coherent increases in the magnitude of CIN over the central and southern Great Plains by 2100 (Fig. 5d).

Following the analyses of Brooks et al. (2003), Trapp et al. (2007), and Gensini and Ashley (2011), the number of days favorable for the formation of severe weather is determined by computing NDSEV. Early-century (2021-2050) changes from the baseline climatology show an increase in boreal spring NDSEV that is especially pronounced over the eastern half of the CONUS, with the largest values over the southeastern U.S. (Fig. 6). Increases in NDSEV continue throughout the rest of this century, yielding values more than double the historical climatology, and largely reflecting spatial patterns evident in CAPE (Fig. 5a). These findings are further evidence that, by 2100, eastern CONUS will likely experience an increase in severe storm activity, despite the robust decrease in projections of S06, especially since the end of century magnitudes of wind shear are still larger than the severe weather threshold (5 ms^{-1}) (Brooks et al., 2003; Trapp et al., 2007, 2009; Diffenbaugh et al., 2013; Hoogewind et al., 2017). While the spatial patterns of change in NDSEV are in broad agreement with previous studies, the magnitude of changes expected by the end of the century are larger than the aforementioned studies. A detailed explanation for these differences is beyond the scope of this paper, but it should be noted

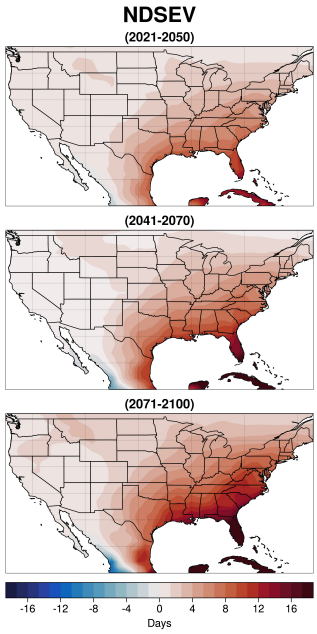

Figure 6. Same as Fig. 5, except for NDSEV (Days).

that other studies used slightly different definitions of NDSEV as well as different models with various forcing scenarios, all of which likely contribute to deviations from the results shown in Fig. 6.

As expressed, the results in this section for CAPE, CIN, S06, and CAPES06 are all in general agreement with previous literature. What makes this work unique is that we have been able to show a robust, multi-century estimate of the large-scale convective environment over the eastern U.S. by using a 50-member ensemble, providing more certainty in the changes of the forced response due to anthropogenic climate change as simulated by the CESM2.

3.2 Internal Variability

Previous studies have primarily focused on changes in convective environments due to anthropogenic climate change (i.e., the forced response). However, the large ensemble approach provides a novel opportunity to investigate the effect of internal (or unforced) climate variability and how it might modify the forced response, where all 50 ensemble members represent an equally possible path to reality. To illustrate the range of possible outcomes, the simple metric of linear trends for each of the convective indices over the next 30 years (2021-2050) is considered. Histograms of the ensemble members are shown in Fig. 7. Changes through 2050 are analyzed because uncertainty due to internal climate variability is most significant over the next several decades relative to the forced signal (Hawkins & Sutton, 2009; Deser, 2020).

Even in the presence of significant internal variability, 30-year trends of boreal spring CAPE over the eastern CONUS are positive for all 50 ensemble members (Fig. 7a), but they exhibit considerable spread. Trends out to 2050 range from near zero to ∼68 $Jkg^{-1}decade^{-1}$, while two-thirds of the ensemble members have CAPE trends between 20 and 40 $Jkg^{-1}decade^{-1}$. Similarly, trends in S06 are mostly of the same sign, with 46 of the 50 ensemble members exhibiting negative trends with a minimum of -0.85 $ms^{-1}decade^{-1}$ projected by four members. These results show that the sign of the response of CAPE and S06 to anthro-

pogenic forcing (Fig. 4a, b) is robust across nearly all of the CESM2-LE members, but that the magnitude of the forced response is likely to be considerably moderated by internal climate variability over the coming decades (Fig. 7a, b). It follows that boreal spring trends in CAPES06 over the coming decades are positive for nearly all ensemble members (Fig. 7c), with 80% of the members exhibiting trends between 100 and 500 $m^3s^{-3}decade^{-1}$. In contrast, the signs of 30-year trends in boreal spring CIN over the eastern CONUS are more mixed (Fig. 7d). Twenty-one of the ensemble members exhibit positive trends, while the other 29 exhibit negative trends down to -4.25 $Jkg^{-1}decade^{-1}$ (Fig. 7d). While Fig. 4d illustrates a forced decrease in CIN magnitudes by the end of the century, the robustness of the sign of the change is less certain due to internal climate variability when averaged over the eastern CONUS (Fig. 7d).

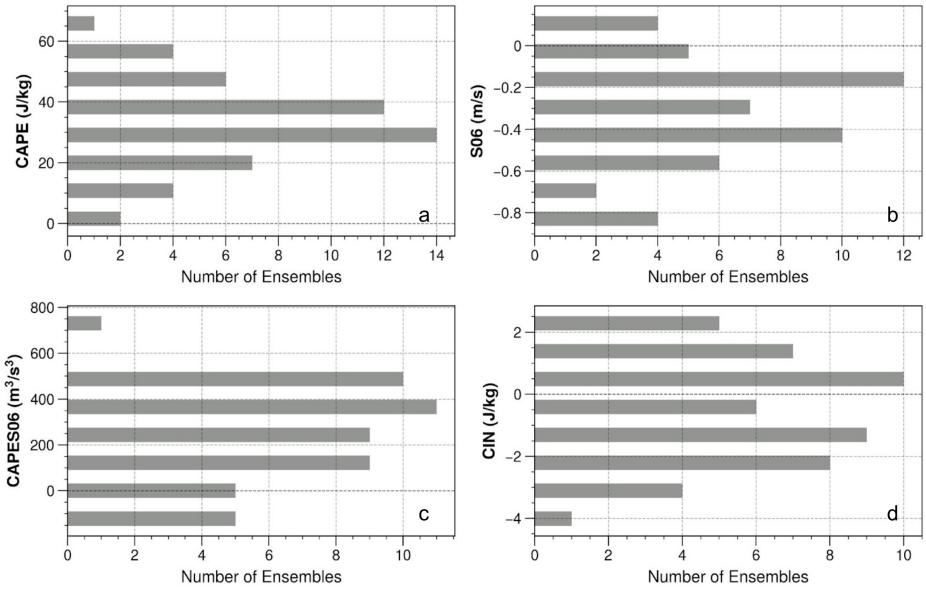

Figure 7. Histograms for 50-member ensemble simulations illustrating the spread of linear trends per decade for the 2021-2050 period during the months March - June for (a.) CAPE ($Jkg^{-1}decade^{-1}$) (b.) S06 ($ms^{-1}decade^{-1}$) (c.) CAPES06 ($m^3s^{-3}decade^{-1}$) (d.) CIN ($Jkg^{-1}decade^{-1}$). Linear trends were calculated using ordinary least squares linear regression and spatial averages were taken over the eastern CONUS region highlighted in Figure 1.

To further illustrate the dominant role that internal climate variability is likely to play over the next several decades, we examine spatial patterns of change by selecting the ensemble members with the largest and smallest trends in area-averaged convective indices over the eastern CONUS during the boreal spring seen in Fig. 7. CAPES06 is discussed since it considers two of the most important elements necessary for severe weather: the thermodynamic energy and kinematic support (Fig. 8).

Ensemble member 25 exhibits the most negative (minimum) CAPES06 trend (-182 $Jkg^{-1}decade^{-1}$) when averaged over the eastern CONUS, while ensemble member 23 has the largest trend (791 $Jkg^{-1}decade^{-1}$) (Fig. 7c). The spatial patterns of the linear decadal trends in CAPES06 for these two simulations are shown in Fig. (8a, d), respectively. By removing the forced trend (ensemble-mean) from each of these individual ensemble members (Fig. 8b, e), the changes in CAPES06 over the next several decades due purely to internal variability are revealed (Fig. 8c, f). In general, the signals of internal climate

variability are spatially coherent and are of a larger magnitude over the next several decades than the forced trends. In ensemble member 25, internal climate variability counteracts the forced, positive change in CAPES06 over much of the southeastern U.S. (Fig. 8c), resulting in an overall negative trend over much of the region (Fig. 8a). Conversely, in ensemble member 23, internal climate variability (Fig. 8f) augments the forced signal and produces a very strong increase through 2050, especially over parts of Texas and the southern Great Plains (Fig. 8d). These two ensemble members were subjectively selected to most dramatically illustrate the role of internal climate variability in modulating the forced response in CAPES06, but a similar approach can be taken with the other ensemble members in Fig. 7 to illustrate the large-scale, coherent spatial patterns of internal variability that significantly modify the forced trend.

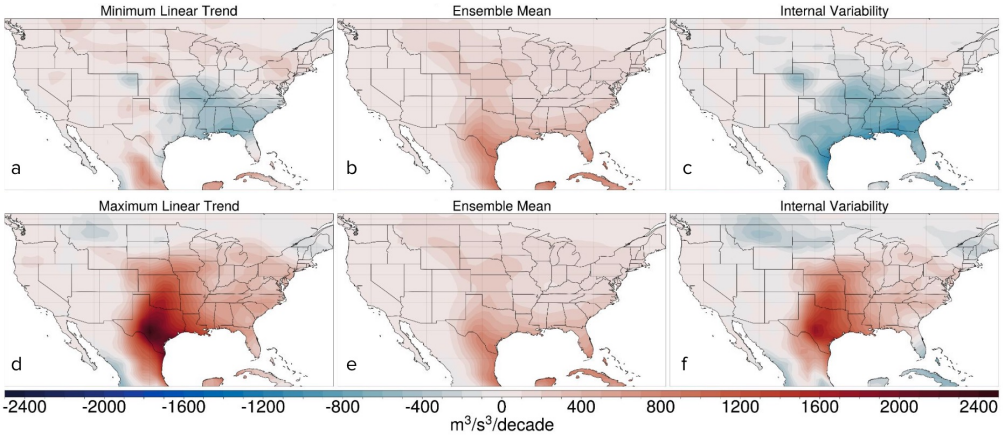

Figure 8. Linear decadal trends for 2021-2050 over the eastern CONUS for the ensemble numbers 25 (top row) and 23 (bottom row) for the full (left; a, d), forced (middle; b, e), and internal (right; c, f) components of MAMJ CAPES06 ($m^3s^{-3}decade^{-1}$).

Similarly, the dominant role of internal variability in affecting NDSEV is illustrated in Fig. 9. On average, over the next several decades (2021-2050), anthropogenic climate change is likely to increase the number of days in boreal spring with convective environments favorable for the development of severe weather over most of the CONUS, with the largest increases over the southeastern U.S. (Fig. 9b, 9e). However, as shown by ensemble member 41 (Fig. 9a), a plausible outcome by 2050 is that internal climate variability could substantially reduce the number of days favorable for severe weather (Fig. 9c). Conversely, ensemble member 23 shows that internal climate variability (Fig. 9f) could augment the increases from climate change, resulting in a large increase in NDSEV by 2050 (Fig. 9d). While internal fluctuations may be considered to be inherently chaotic and random, they are a product of the large-scale dynamics and thus, are spatially coherent with relatively large magnitudes (Fig. 8, 9). Further examining the circulation anomalies that drive such internal variations in these convective parameters is the subject of future work. A key point is that when considering future projections of greenhouse-gas forced changes in severe weather environments, the extent to which they will be modulated by internal variability is important to consider.

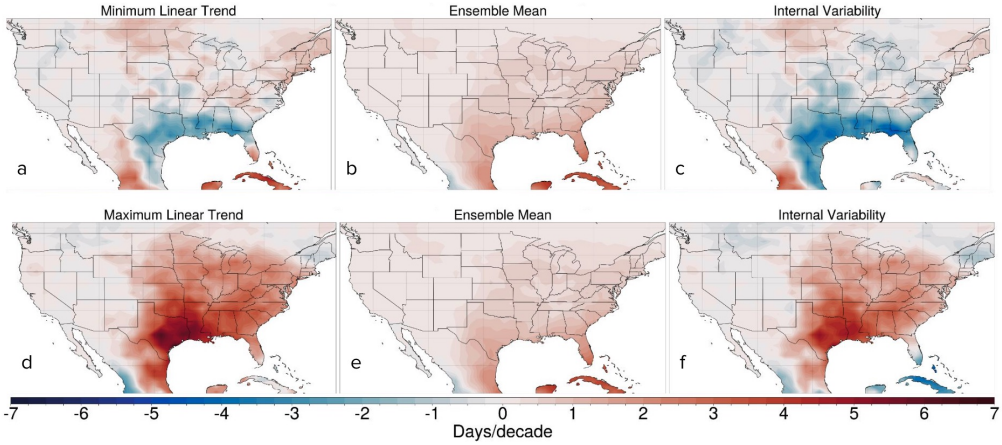

Figure 9. Linear decadal trends for 2021-2050 over the eastern CONUS for the ensemble numbers 41 (top row) and 23 (bottom row) for the full (left; a, d), forced (middle; b, e), and internal (right; c, f) components of MAMJ NDSEV (Daysdecade^{-1}).

In addition to employing covariate proxies, epoch bivariate distribution plots, or two-dimensional histograms, were created to examine the future phase spaces (i.e., convective frequency and intensity) of various convective indices, due to both forced and internal variability, to gain more insight into changes in the convective mode. As mentioned earlier, K. L. Rasmussen et al. (2017) used dynamical downscaling to produce convection-permitting regional climate model projections of end-of-century (2071-2100) May-June CAPE and CIN over the Midwest to examine changes in the thermodynamic environment. By producing a two-dimensional histogram, they found that by the end of the century, convective environments are increasingly characterized by higher average CAPE ($\sim$400 Jkg^{-1}) and lower average (or increased) CIN ($\sim$ -80 Jkg^{-1}) indicative of more vigorous convective storms but a stronger capping inversion. We have taken a similar approach using the CESM2-LE to illustrate changes in both the forced and internal components of the convective indices over time. The bivariate distributions of the historical climatology (1971-2000, blue) and future 30-year periods (2021-2050, orange; and 2071-2100, green) are shown in Fig. 10. Individual, or marginal, distributions are displayed on the opposite axis for each index, helping to highlight the range due to internal variability, and how it changes through the century. While the shape of the distribution gives some insight into the range of internal variability, the shifts in the CAPE versus CIN pattern as a whole are due to the changes over time in the forced response.

For the late 20th century (blue), the distribution in Fig. 10a has the highest density of ensemble members around CAPE values of 440 Jkg^{-1} and CIN values around -29 Jkg^{-1}. Over the next several decades (orange), the distribution exhibits an overall shift toward the bottom right of the diagram with relatively higher CAPE (560 Jkg^{-1}) and relatively lower, or increased magnitudes, of CIN (-36 Jkg^{-1}). By the end of the 21st century (green), the CAPE versus CIN distribution has shifted to even higher CAPE and lower CIN, with average magnitudes of $\sim$ 745 Jkg^{-1} and -40 Jkg^{-1}, respectively (Fig. 10a). In Fig. 10a, the shape of the end-of-century epoch (green) indicates that the future projections of CAPE could be anywhere from approximately 500 to 1050 Jkg^{-1} by the end of the century. Conversely, even with an ensemble mode of -40 Jkg^{-1}, the range of future projections for CIN due to the internal variability could fall anywhere between -26 and -70 Jkg^{-1} (Fig. 10a). Thus, even though a wide range of plausible outcomes exist for both CAPE and CIN due to the role of internal variability, a majority of the ensemble members suggest future environments over the southeastern CONUS will be com-

posed of higher CAPE and increased magnitudes of CIN compared to the present-day climate (Diffenbaugh et al., 2013; K. L. Rasmussen et al., 2017; Lepore et al., 2021). The balance between these two thermodynamic indices is key to determining future convective modes and frequency (Diffenbaugh et al., 2013; K. L. Rasmussen et al., 2017; Chen et al., 2020; Lepore et al., 2021).

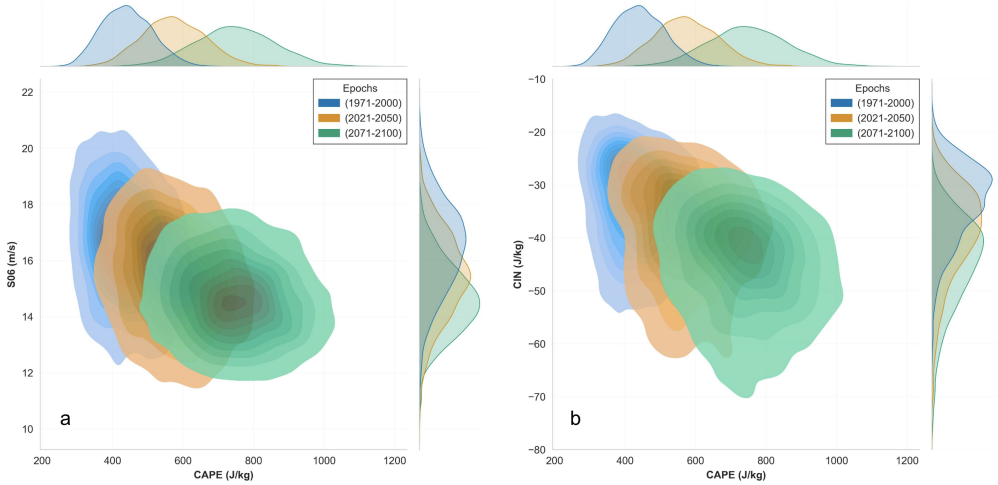

Figure 10. Bivariate distributions over eastern CONUS for MAMJ (a.) CAPE (Jkg^{-1}) vs. CIN (Jkg^{-1}) and (b.) CAPE (Jkg^{-1}) vs. S06 (ms^{-1}) for various epochs: 1971-2000 in blue, 2021-2050 in orange, and 2071-2100 in green. Marginal distributions for each index and period are shown on the opposite axis.

The same analysis can be done for the CAPE and vertical wind shear phase space (Fig. 10b), which is key for storm type and organization. Overall, the phase space of these two indices shifts from relatively moderate CAPE and high S06 to higher CAPE and lower S06 (Trapp et al., 2007; Diffenbaugh et al., 2013; Hoogewind et al., 2017; Lepore et al., 2021). The CAPE distributions are the same as Fig. 10a, but the distribution in bulk vertical wind shear follows a decreasing trend throughout the century, with an ensemble mode of approximately 14.5 ms^{-1} by 2100 (Fig. 10b, green). It is also clear that, from the historical climatology to the end of the century, the shapes of the epochs evolve from long and narrow to a more circular shape. In other words, the uncertainty in S06 changes due to internal variability is likely to decrease as the century progresses, whereas the uncertainty in changes to CAPE is likely to increase. Previously, Brooks et al. (2003) analyzed soundings from reanalysis data that were associated with severe thunderstorms in the U.S. from 1997-1999. These soundings were further classified as little severe, significant severe, and significant tornadoes. Their two-dimensional histogram of CAPE and S06 indicated the most severe storms were characterized by high CAPE and high wind shear (i.e., the top right of Fig. 10b). Further, the storms that were classified as significant tornadoes had S06 greater than 10 ms^{-1}, and storms that were classified as significant severe exhibited S06 greater than 5 ms^{-1}. The distribution for significant severe storms existed over the high CAPE region (100-5000 Jkg^{-1}), but significant tornadoes exhibited values across the full range of CAPE distributions.

Comparing our results to the storm classifications in Brooks et al. (2003) and other studies (E. N. Rasmussen & Blanchard, 1998; Brooks, 2009), the projected increases in end-of-century CAPE will be more than sufficient to support significant severe storms and tornadoes. Although, while S06 is projected to decrease, even in the presence of in-

ternal variability, the absolute magnitudes of wind shear (Fig. 10b) remain above the threshold to produce significant severe weather, but may not be as supportive of the most intense types of severe weather (e.g. tornadoes or derechos). The implication of higher CAPE and lower S06 is that when future storms do occur, there is a smaller chance that they will have the necessary dynamical support and organization to produce the most intense severe weather compared to the current climate, paralleling past research (Diffenbaugh et al., 2013; Lepore et al., 2021).

4 Discussion and Conclusion

An important goal of this study was to better understand how severe and hazardous weather is likely to change in a warmer, future climate. While the spatiotemporal scales on which severe storms form are smaller than can be explicitly resolved by relatively coarse resolution models such as the CESM2, such models can be leveraged to instead examine the evolution of the large-scale convective environments in which the storms develop. Further, by using a large ensemble of climate model simulations as we have done with the CESM2-LE, it is possible to not only identify and examine anthropogenically-forced changes in convective environments over time but also how the forced changes are likely to be altered by internal climate variability. This latter aspect, to our knowledge, has yet to be robustly documented. An increased understanding of the range of plausible, future convective environments can enhance our capability to better project the nature of severe weather in the future, and perhaps increase resilience to these hazards.

Our study is novel in that we have examined the continuous-time evolution of various convective indices from 1870-2100 over the CONUS using a 50-member ensemble from a well-documented and understood Earth system model. By using a large ensemble from a single model, we were able to obtain a robust estimate of the forced response. Our results are in agreement with previous studies that anthropogenic climate change will likely drive future convective environments over the eastern U.S. toward less frequent, but more intense and deep convection. Additionally, there will also be less kinematic support, which means less support for the organization of supercells and other multi-cellular convective storm modes capable of delivering the most extreme severe weather risks.

By taking advantage of a large ensemble approach, this study was further able to robustly investigate the effect of internal climate variability on large-scale convective environments, rather than just the forced response as most previous studies have done. While we have shown that the end-of-century changes in convective environments due to the forced response are spatially coherent and robust, we have also demonstrated how these changes can be substantially modulated by internal variability. The latter has spatial coherency and thus can either significantly enhance or suppress the forced changes.

Examining the convective proxies and the bivariate distributions of the selected indices, it is likely that future environments will be characterized by higher CAPE, moderate-high magnitudes of CIN, and lower S06, which is in general agreement with previous literature. Our results thus suggest that there will be an increase in frequency in the less severe convective modes such as multi-cellular and ordinary thunderstorms. The actual time evolution of these quantities will, of course, not only be influenced by forced climate change, but also by internal variability. While it is not possible to make a deterministic prediction of how actual convective environments over the CONUS will evolve throughout the rest of this century, our study has helped to quantify the range of uncertainty and plausible scenarios.

Our conclusions depend on the assumption that the CESM2-LE is capable of accurately simulating the future, even though it performs well in simulating past convective environments (e.g., Figs. 2, 3). Our results are also dependent on the future forcing scenario (SSP3-7.0) used to produce the CESM2-LE.

This study is the first to exploit the CESM2-LE to examine changes in convective parameters. Plans for future work include more comprehensive regional analyses, especially since some regions are less influenced by internal variability than others (Deser et al., 2012b), and in this study, averages have been taken over a very large spatial domain (Fig. 1). Also, given the prominent and coherent role of internal variability over the southeastern U.S., further analysis is necessary to examine the large-scale circulation changes that drive internal variations in the convective indices, and if those circulation changes are connected to large-scale coupled modes of climate variability. If so, it will be important to determine the level of predictability associated with internal variability. Finally, similar analyses for other seasons, as well as other regions of the world where convective activity is pronounced, such as over Argentina on the lee-side of the Andes (e.g., Zipser et al., 2006; K. L. Rasmussen & Houze, 2011; K. L. Rasmussen et al., 2014; Mulholland et al., 2018; Nesbitt et al., 2021) are underway. A better understanding of the possible future evolution and variability in large-scale convective environments is critical for understanding future changes in severe weather hazards and in particular, how we choose to adapt to these hazards.

Open Research Section

The first 50 ensemble members from The Community Earth System Model Version 2-Large Ensemble data (CESM2-LE; Danabasoglu et al., 2020; Rodgers et al., 2021) used for this study can be found and downloaded publicly online at `https://doi.org/10.26024/kgmp-c556`. Data from the Fifth-Generation Global Climate Reanalysis (ERA5; Hersbach et al., 2020) can also be found and downloaded publicly online at `https://doi.org/10.5065/BH6N-5N20`.

Acknowledgments

We would like to acknowledge the CESM2 Large Ensemble Community Project and supercomputing resources provided by the IBS Center for Climate Physics in South Korea. In addition, we would also like to acknowledge Dan Chavas of Purdue University for preliminary conversations regarding this project, as well as for providing us with the calculated ERA5 convective parameters used in this study. Thank you to the listed co-authors for their support and guidance in completing this project as well as to the Department of Atmospheric Science and the Walter Scott, Jr. College of Engineering at Colorado State University.

References

Allen, J. T., Tippett, M. K., & Sobel, A. H. (2015). Influence of the El Niño/Southern Oscillation on tornado and hail frequency in the United States. *Nature Geoscience*, *8*(4), 278–283. doi: 10.1038/ngeo2385

Brooks, H. E. (2009). Proximity soundings for severe convection for Europe and the United States from reanalysis data. *Atmospheric Research*, *93*, 546–553. doi: 10.1016/j.atmosres.2008.10.005

Brooks, H. E., Lee, J. W., & Craven, J. P. (2003). The spatial distribution of severe thunderstorm and tornado environments from global reanalysis data. *Atmospheric Research*, *67-68*, 73–94. doi: 10.1016/S0169-8095(03)00045-0

Capotondi, A., Deser, C., Phillips, A. S., Okumura, Y., & Larson, S. M. (2020). ENSO and Pacific Decadal Variability in the Community Earth System Model Version 2. *Journal of Advances in Modeling Earth Systems*, *12*(12), e2019MS002022. doi: 10.1029/2019MS002022

Carlson, T. N., Benjamin, S. G., Forbes, G. S., & Li, Y.-F. (1983). Elevated Mixed Layers in the Regional Severe Storm Environment: Conceptual Model and Case Studies. *Monthly Weather Review*, *111*(7), 1453–1474. doi:

10.1175/1520-0493(1983)111⟨1453:EMLITR⟩2.0.CO;2

Chen, J., Dai, A., Zhang, Y., & Rasmussen, K. L. (2020). Changes in Convective Available Potential Energy and Convective Inhibition under Global Warming. *Journal of Climate*, *33*(6), 2025–2050. doi: 10.1175/JCLI-D-19-0461.1

Colby, F. P. (1984). Convective Inhibition as a Predictor of Convection during AVE-SESAME II. *Monthly Weather Review*, *112*(11), 2239–2252. doi: 10.1175/1520-0493(1984)112⟨2239:CIAAPO⟩2.0.CO;2

Craven, J. P., & Brooks, H. E. (2004). Baseline Climatology of Sounding Derived Parameters Associated With Deep Moist Convection. *National Weather Digest*, *28*, 13–24. `https://www.nssl.noaa.gov/users/brooks/public_html/papers/cravenbrooksnwa.pdf`.

Craven, J. P., Jewell, R. E., & Brooks, H. E. (2002). Comparison between Observed Convective Cloud-Base Heights and Lifting Condensation Level for Two Different Lifted Parcels. *Weather and Forecasting*, *17*(4), 885–890. doi: 10.1175/1520-0434(2002)017⟨0885:CBOCCB⟩2.0.CO;2

Dai, A., Fung, I. Y., & Genio, A. D. D. (1997). Surface Observed Global Land Precipitation Variations during 1900–88. *Journal of Climate*, *10*(11), 2943–2962. doi: 10.1175/1520-0442(1997)010⟨2943:SOGLPV⟩2.0.CO;2

Dai, A., & Wigley, T. M. L. (2000). Global patterns of ENSO-induced precipitation. *Geophysical Research Letters*, *27*(9), 1283–1286. doi: 10.1029/1999GL011140

Danabasoglu, G., Lamarque, J.-F., Bacmeister, J., Bailey, D. A., DuVivier, A. K., Edwards, J., et al. (2020). The Community Earth System Model Version 2 (CESM2). *Journal of Advances in Modeling Earth Systems*, *12*(2), e2019MS001916. doi: 10.1029/2019MS001916

Deser, C. (2020). "Certain Uncertainty: The Role of Internal Climate Variability in Projections of Regional Climate Change and Risk Management". *Earth's Future*, *8*(12), e2020EF001854. doi: 10.1029/2020EF001854

Deser, C., Knutti, R., Solomon, S., & Phillips, A. S. (2012b). Communication of the role of natural variability in future North American climate. *Nature Climate Change*, *2*(11). doi: 10.1038/nclimate1562

Deser, C., Phillips, A., Bourdette, V., & Teng, H. (2012a). Uncertainty in climate change projections: the role of internal variability. *Climate Dynamics*, *38*(3), 527–546. doi: 10.1007/s00382-010-0977-x

Diffenbaugh, N. S., Scherer, M., & Trapp, R. J. (2013). Robust increases in severe thunderstorm environments in response to greenhouse forcing. *Proceedings of the National Academy of Sciences*, *110*(41), 16361–16366. doi: 10.1073/pnas.1307758110

Doswell, C. A., & Rasmussen, E. N. (1994). The Effect of Neglecting the Virtual Temperature Correction on CAPE Calculations. *Weather and Forecasting*, *9*(4), 625–629. doi: 10.1175/1520-0434(1994)009⟨0625:TEONTV⟩2.0.CO;2

Dougherty, E., & Rasmussen, K. L. (2021). Variations in Flash Flood–Producing Storm Characteristics Associated with Changes in Vertical Velocity in a Future Climate in the Mississippi River Basin. *Journal of Hydrometeorology*, *22*(3), 671–687. doi: 10.1175/JHM-D-20-0254.1

Eyring, V., Bony, S., Meehl, G. A., Senior, C. A., Stevens, B., Stouffer, R. J., & Taylor, K. E. (2016). Overview of the Coupled Model Intercomparison Project Phase 6 (CMIP6) experimental design and organization. *Geoscientific Model Development*, *9*(5), 1937–1958. doi: 10.5194/gmd-9-1937-2016

Gensini, V. A., & Ashley, W. S. (2011). Climatology of Potentially Severe Convective Environments from the North American Regional Reanalysis. *Electronic J. Severe Storms Meteor*, *6*(8), 1-40. doi: 10.55599/ejssm.v6i8.35

Gettelman, A., & Morrison, H. (2015). Advanced Two-Moment Bulk Microphysics for Global Models. Part I: Off-Line Tests and Comparison with Other Schemes. *Journal of Climate*, *28*(3), 1268–1287. doi: 10.1175/JCLI-D-14-00102.1

Golaz, J.-C., Larson, V. E., & Cotton, W. R. (2002). A PDF-Based Model for Boundary Layer Clouds. Part I: Method and Model Description. *Journal of the Atmospheric Sciences*, *59*(24), 3540–3551. doi: 10.1175/1520-0469(2002)059⟨3540:APBMFB⟩2.0.CO;2

Hawkins, E., & Sutton, R. (2009). The Potential to Narrow Uncertainty in Regional Climate Predictions. *Bulletin of the American Meteorological Society*, *90*(8), 1095–1108. doi: 10.1175/2009BAMS2607.1

Hersbach, H., Bell, B., Berrisford, P., Hirahara, S., Horányi, A., Muñoz-Sabater, J., ... Thépaut, J.-N. (2020). The ERA5 global reanalysis. *Quarterly Journal of the Royal Meteorological Society*, *146*(730), 1999–2049. doi: 10.1002/qj.3803

Higgins, R. W., Yao, Y., Yarosh, E. S., Janowiak, J. E., & Mo, K. C. (1997). Influence of the Great Plains Low-Level Jet on Summertime Precipitation and Moisture Transport over the Central United States. *Journal of Climate*, *10*(3), 481–507. doi: 10.1175/1520-0442(1997)010⟨0481:IOTGPL⟩2.0.CO;2

Holton, J. R., & Hakim, G. J. (2013). Chapter 9 - Mesoscale Circulations. In *An Introduction to Dynamic Meteorology* (Fifth ed., p. 279-323). Boston: Academic Press. doi: 10.1016/B978-0-12-384866-6.00009-X

Hoogewind, K. A., Baldwin, M. E., & Trapp, R. J. (2017). The Impact of Climate Change on Hazardous Convective Weather in the United States: Insight from High-Resolution Dynamical Downscaling. *Journal of Climate*, *30*(24), 10081–10100. doi: 10.1175/JCLI-D-16-0885.1

Hurrell, J. W., Holland, M. M., Gent, P. R., Ghan, S., Kay, J. E., Kushner, P. J., ... Marshall, S. (2013). The Community Earth System Model: A Framework for Collaborative Research. *Bulletin of the American Meteorological Society*, *94*(9), 1339–1360. doi: 10.1175/BAMS-D-12-00121.1

IPCC. (2021). Summary for policymakers. In *Climate Change 2021: The Physical Science Basis. Contribution of Working Group I to the Sixth Assessment Report of the Intergovernmental Panel on Climate Change* (p. 332). Cambridge, United Kingdom and New York, NY, USA: Cambridge University Press. doi: 10.1017/9781009157896.001

Johns, R. H., & Doswell, C. A. (1992). Severe Local Storms Forecasting. *Weather and Forecasting*, *7*(4), 588–612. doi: 10.1175/1520-0434(1992)007⟨0588:SLSF⟩2.0.CO;2

Kelly, D. L., Schaefer, J. T., & Doswell, C. A. (1985). Climatology of Nontornadic Severe Thunderstorm Events in the United States. *Monthly Weather Review*, *113*(11), 1997–2014. doi: 10.1175/1520-0493(1985)113⟨1997:CONSTE⟩2.0.CO;2

Kirtman, B. P., Min, D., Infanti, J. M., Kinter, J. L., Paolino, D. A., Zhang, Q., ... Wood, E. F. (2014). The North American Multimodel Ensemble: Phase-1 Seasonal-to-Interannual Prediction; Phase-2 toward Developing Intraseasonal Prediction. *Bulletin of the American Meteorological Society*, *95*(4), 585–601. doi: 10.1175/BAMS-D-12-00050.1

Klemp, J. B. (1987). Dynamics of Tornadic Thunderstorms. *Annual Review of Fluid Mechanics*, *19*(1), 369–402. doi: 10.1146/annurev.fl.19.010187.002101

Lee, S.-K., Atlas, R., Enfield, D., Wang, C., & Liu, H. (2013). Is There an Optimal ENSO Pattern That Enhances Large-Scale Atmospheric Processes Conducive to Tornado Outbreaks in the United States? *Journal of Climate*, *26*(5), 1626–1642. doi: 10.1175/JCLI-D-12-00128.1

Lepore, C., Abernathey, R., Henderson, N., Allen, J. T., & Tippett, M. K. (2021). Future Global Convective Environments in CMIP6 Models. *Earth's Future*, *9*(12), e2021EF002277. doi: 10.1029/2021EF002277

Li, F., Chavas, D. R., Reed, K. A., & Dawson II, D. T. (2020). Climatology of Severe Local Storm Environments and Synoptic-Scale Features over North America in ERA5 Reanalysis and CAM6 Simulation. *Journal of Climate*, *33*(19), 8339–8365. doi: 10.1175/JCLI-D-19-0986.1

Li, W., Li, L., Fu, R., Deng, Y., & Wang, H. (2011). Changes to the North Atlantic Subtropical High and Its Role in the Intensification of Summer Rainfall Variability in the Southeastern United States. *Journal of Climate*, *24*(5), 1499–1506. doi: 10.1175/2010JCLI3829.1

Lilly, D. K. (1979). The Dynamical Structure and Evolution of Thunderstorms and Squall Lines. *Annual Review of Earth and Planetary Sciences*, *7*, 117. doi: 10.1146/annurev.ea.07.050179.001001

Liu, C., Ikeda, K., Rasmussen, R., Barlage, M., Newman, A. J., Prein, A. F., ... Yates, D. (2017). Continental-scale convection-permitting modeling of the current and future climate of North America. *Climate Dynamics*, *49*(1), 71–95. doi: 10.1007/s00382-016-3327-9

Ludlam, F. H. (1963). Severe Local Storms: A Review. In *Severe Local Storms Meteorological Monographs* (Vol. 5, pp. 1–32). American Meteorological Society. doi: 10.1007/978-1-940033-56-3_1

Mankin, J. S., Lehner, F., Coats, S., & McKinnon, K. A. (2020). The Value of Initial Condition Large Ensembles to Robust Adaptation Decision-Making. *Earth's Future*, *8*(10). doi: 10.1029/2020EF001610

Milinski, S., Maher, N., & Olonscheck, D. (2020). How large does a large ensemble need to be? *Earth System Dynamics*, *11*(4), 885–901. doi: 10.5194/esd-11-885-2020

Mulholland, J. P., Nesbitt, S. W., Trapp, R. J., Rasmussen, K. L., & Salio, P. V. (2018). Convective Storm Life Cycle and Environments near the Sierras de Córdoba, Argentina. *Monthly Weather Review*, *146*(8), 2541–2557. doi: 10.1175/MWR-D-18-0081.1

NCEI. (2021). Noaa National Centers for Environmental Information (NCEI) U.S. Billion-Dollar Weather and Climate Disasters. doi: 10.25921/stkw-7w73

Neale, R. B., & Gettelman, A. (2012). Description of the NCAR Community Atmosphere Model (CAM 5.0) (No. NCAR/TN-486+STR). University Corporation for Atmospheric Research. doi: 10.5065/wgtk-4g06

Nesbitt, S. W., Salio, P. V., Ávila, E., Bitzer, P., Carey, L., Chandrasekar, V., ... Grover, M. A. (2021). A Storm Safari in Subtropical South America: Proyecto RELAMPAGO. *Bulletin of the American Meteorological Society*, *102*(8), E1621–E1644. doi: 10.1175/BAMS-D-20-0029.1

O'Neill, B. C., Tebaldi, C., van Vuuren, D. P., Eyring, V., Friedlingstein, P., Hurtt, G., ... Sanderson, B. M. (2016). The Scenario Model Intercomparison Project (ScenarioMIP) for CMIP6. *Geoscientific Model Development*, *9*(9), 3461–3482. doi: 10.5194/gmd-9-3461-2016

Otto-Bliesner, B. L., Brady, E. C., Fasullo, J., Jahn, A., Landrum, L., Stevenson, S., ... Strand, G. (2016). Climate Variability and Change since 850 CE: An Ensemble Approach with the Community Earth System Model. *Bulletin of the American Meteorological Society*, *97*(5), 735–754. doi: 10.1175/BAMS-D-14-00233.1

Pitchford, K. L., & London, J. (1962). The Low-Level Jet as Related to Nocturnal Thunderstorms over Midwest United States. *Journal of Applied Meteorology and Climatology*, *1*(1), 43–47. doi: 10.1175/1520-0450(1962)001⟨0043:TLLJAR⟩2.0.CO;2

Rasmussen, E. N., & Blanchard, D. O. (1998). A Baseline Climatology of Sounding-Derived Supercell and Tornado Forecast Parameters. *Weather and Forecasting*, *13*(4), 1148–1164. doi: 10.1175/1520-0434(1998)013⟨1148:ABCOSD⟩2.0.CO;2

Rasmussen, K. L., & Houze, R. A. (2011). Orogenic Convection in Subtropical South America as Seen by the TRMM Satellite. *Monthly Weather Review*, *139*(8), 2399–2420. doi: 10.1175/MWR-D-10-05006.1

Rasmussen, K. L., & Houze, R. A. (2016). Convective Initiation near the Andes in Subtropical South America. *Monthly Weather Review*, *144*(6), 2351–2374. doi: 10.1175/MWR-D-15-0058.1

Rasmussen, K. L., Prein, A. F., Rasmussen, R. M., Ikeda, K., & Liu, C. (2017). Changes in the convective population and thermodynamic environments in convection-permitting regional climate simulations over the United States. *Climate Dynamics*, *55*(1), 383–408. doi: 10.1007/s00382-017-4000-7

Rasmussen, K. L., Zuluaga, M. D., & Houze Jr., R. A. (2014). Severe convection and lightning in subtropical south america. *Geophysical Research Letters*, *41*(20), 7359-7366. doi: 10.1002/2014GL061767

Riemann-Campe, K., Fraedrich, K., & Lunkeit, F. (2009). Global climatology of Convective Available Potential Energy (CAPE) and Convective Inhibition (CIN) in ERA-40 reanalysis. *Atmospheric Research*, *93*(1), 534–545. doi: 10.1016/j.atmosres.2008.09.037

Rochette, S. M., Moore, J. T., & Market, P. S. (1999). The importance of parcel choice in elevated CAPE computations. *Natl. Wea. Dig*, *23*(4), 20–32.

Rodgers, K. B., Lee, S.-S., Rosenbloom, N., Timmermann, A., Danabasoglu, G., Deser, C., et al. (2021). Ubiquity of human-induced changes in climate variability. *Earth System Dynamics*, *12*(4), 1393–1411. doi: 10.5194/esd-12-1393-2021

Ropelewski, C. F., & Halpert, M. S. (1986). North American Precipitation and Temperature Patterns Associated with the El Niño/Southern Oscillation (ENSO). *Monthly Weather Review*, *114*(12), 2352–2362. doi: 10.1175/1520-0493(1986)114⟨2352:NAPATP⟩2.0.CO;2

Rotunno, R. (1981). On the Evolution of Thunderstorm Rotation. *Monthly Weather Review*, *109*(3), 577–586. doi: 10.1175/1520-0493(1981)109⟨0577:OTEOTR⟩2.0.CO;2

Rotunno, R., Klemp, J. B., & Weisman, M. L. (1988). A Theory for Strong, Long-Lived Squall Lines. *Journal of the Atmospheric Sciences*, *45*(3), 463–485. doi: 10.1175/1520-0469(1988)045⟨0463:ATFSLL⟩2.0.CO;2

Seeley, J. T., & Romps, D. M. (2015). The Effect of Global Warming on Severe Thunderstorms in the United States. *Journal of Climate*, *28*(6), 2443–2458. doi: 10.1175/JCLI-D-14-00382.1

Skamarock, W. C., Klemp, J. B., Dudhia, J., Gill, D. O., Barker, D. M., Duda, M. G., ... Powers, J. G. (2008). A Description of the Advanced Research WRF Version 3 (No. NCAR/TN-475+STR). University Corporation for Atmospheric Research.
doi: 10.5065/D68S4MVH

Taszarek, M., Allen, J. T., Marchio, M., & Brooks, H. E. (2021). Global climatology and trends in convective environments from ERA5 and rawinsonde data. *npj Climate and Atmospheric Science*, *4*(1), 1–11. doi: 10.1038/s41612-021-00190-x

Taylor, K. E., Stouffer, R. J., & Meehl, G. A. (2012). An Overview of CMIP5 and the Experiment Design. *Bulletin of the American Meteorological Society*, *93*(4), 485–498. doi: 10.1175/BAMS-D-11-00094.1

Thompson, D. B., & Roundy, P. E. (2013). The Relationship between the Madden–Julian Oscillation and U.S. Violent Tornado Outbreaks in the Spring. *Monthly Weather Review*, *141*(6), 2087–2095. doi: 10.1175/MWR-D-12-00173.1

Ting, M., Kossin, J. P., Camargo, S. J., & Li, C. (2019). Past and Future Hurricane Intensity Change along the U.S. East Coast. *Scientific Reports*, *9*(1), 7795. doi: 10.1038/s41598-019-44252-w

Trapp, R. J., Diffenbaugh, N. S., Brooks, H. E., Baldwin, M. E., Robinson, E. D., & Pal, J. S. (2007). Changes in severe thunderstorm environment frequency during the 21st century caused by anthropogenically enhanced global radiative

forcing. *Proceedings of the National Academy of Sciences*, *104*(50), 19719–19723. doi: 10.1073/pnas.0705494104

Trapp, R. J., Diffenbaugh, N. S., & Gluhovsky, A. (2009). Transient response of severe thunderstorm forcing to elevated greenhouse gas concentrations. *Geophysical Research Letters*, *36*(1). doi: 10.1029/2008GL036203

Weisman, M. L., & Rotunno, R. (2000). The Use of Vertical Wind Shear versus Helicity in Interpreting Supercell Dynamics. *Journal of the Atmospheric Sciences*, *57*(9), 1452–1472. doi: 10.1175/1520-0469(2000)057⟨1452:TUOVWS⟩2.0.CO;2

Zhang, G., & McFarlane, N. A. (1995). Sensitivity of climate simulations to the parameterization of cumulus convection in the Canadian climate centre general circulation model. *Atmosphere-Ocean*, *33*(3), 407–446. doi: 10.1080/07055900.1995.9649539

Zipser, E. J., Cecil, D. J., Liu, C., Nesbitt, S. W., & Yorty, D. P. (2006). WHERE ARE THE MOST INTENSE THUNDERSTORMS ON EARTH? *Bulletin of the American Meteorological Society*, *87*(8), 1057–1072. doi: 10.1175/BAMS-87-8-1057